
Photoelectron Spectroscopy of Reactive Intermediates

V. Butcher, M. C. R. Cockett, J. M. Dyke, A. M. Ellis, M. Feher, A. Morris and H. Zamanpour

Phil. Trans. R. Soc. Lond. A 1988 **324**, 197-207
doi: 10.1098/rsta.1988.0011

Email alerting service

Receive free email alerts when new articles cite this article - sign up in the box at the top right-hand corner of the article or click [here](#)

To subscribe to *Phil. Trans. R. Soc. Lond. A* go to: <http://rsta.royalsocietypublishing.org/subscriptions>

Photoelectron spectroscopy of reactive intermediates

BY V. BUTCHER, M. C. R. COCKETT, J. M. DYKE, A. M. ELLIS, M. FEHER,
A. MORRIS AND H. ZAMANPOUR

Department of Chemistry, University of Southampton, Southampton SO9 5NH, U.K.

Recent developments in the use of photoelectron spectroscopy to study reactive intermediates in the gas phase are reviewed. The information to be derived on low-lying cationic states from such studies is illustrated by considering two diatomic molecules, NCl and PF, and one triatomic molecule, HNO.

Also, the use of a transition-metal photoelectron spectrum to interpret the photoelectron spectrum of the corresponding transition-metal oxide is discussed by using the spectra of vanadium and vanadium monoxide as examples. The value of superheating in high-temperature photoelectron spectroscopy is demonstrated by considering the vapour-phase photoelectron spectra of the monomers and dimers of sodium hydroxide.

Unlike most of the other contributions to this Meeting where the aim is to prepare molecular ions in sufficient concentration for spectroscopic study, the work described in this paper is based on generating unstable molecules in sufficient concentrations in the gas phase for study by photoelectron spectroscopy (PES) (Dyke *et al.* 1979, 1982*c*; Dyke 1987).

If a photon removes an electron from a molecule, then measurement of the kinetic energy of the electrons produced combined with the conservation-of-energy condition means that the ionization energy of the molecule can be determined. This can be summarized as

$$M + h\nu \rightarrow M^+ + e^-, \quad (1)$$

$$KE(e^-) = h\nu - I_n - \Delta E_{\text{vib}}, \quad (2)$$

where M is the molecule under consideration, ΔE_{vib} is the change in vibrational energy on ionization and I_n is the ionization energy corresponding to the separation of the zeroth vibrational levels in the molecule and ion. In general terms, through measurement of I_n and ΔE_{vib} the PES technique is capable of providing information on electronic states of molecular ions that are accessible from the neutral molecule by one-electron ionization, although if the neutral molecule is electronically or vibrationally excited, information on the neutral species may be obtained.

One way of generating an excited state of a molecule is via a microwave discharge of a flowing gas mixture. For example, microwave discharging molecular oxygen excites some $O_2(X^3\Sigma_g^-)$ to $O_2(a^1\Delta_g)$ and one-electron ionization of $O_2(a^1\Delta_g)$ gives some states of O_2^+ that are not seen on one-electron ionization of $(O_2X^3\Sigma_g^-)$ (Jonathan *et al.* 1974).

Another way of populating an excited state of a molecule is via an exothermic chemical reaction. For example, NF is isoelectronic with O_2 , and its first excited state, the $a^1\Delta$ state, can be produced from the reaction of fluorine atoms with the N_3 radical, which in turn can be produced from the reaction of fluorine atoms with HN_3 (Dyke *et al.* 1982*a, b*), i.e.



[123]

Both of these reactions are known to be rapid at room temperature (Pritt & Coombe 1980) and the $F+N_3$ reaction is sufficiently exothermic to populate both the $X^3\Sigma^-$ and $a^1\Delta$ states of NF.

Bands associated with ionization of both states can be seen in the experimental photoelectron spectrum recorded for the products of this reaction (see figure 1). The first ionization process

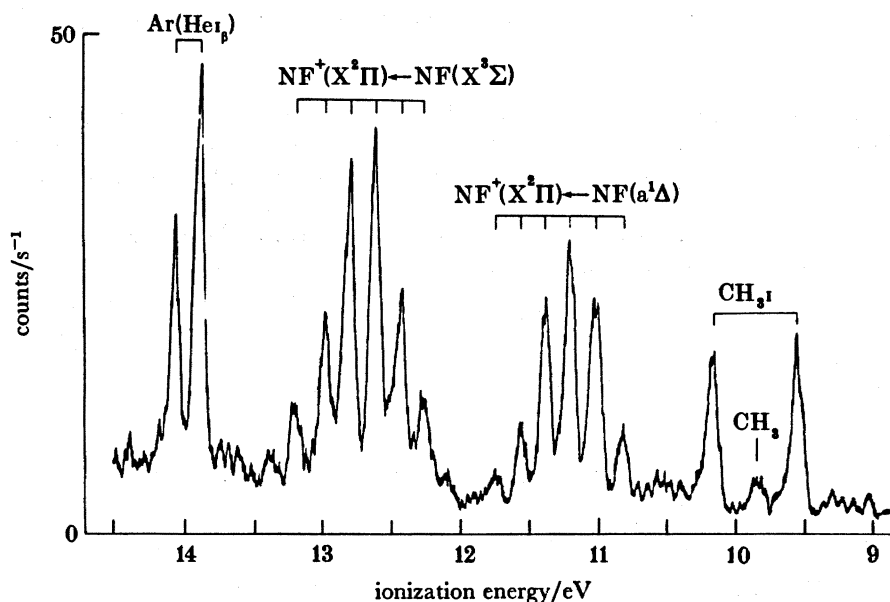


FIGURE 1. Part of the HeI photoelectron spectrum observed for the $F+N_3$ reaction.

for both the $NF(X^3\Sigma^-)$ and $NF(a^1\Delta)$ states corresponds to removal of an electron from the outermost filled orbital, a π -antibonding molecular orbital, to give the $NF^+(X^2\Pi)$ state. Measurement of the vibrational component separations in each band allows a value of the vibrational constant, $\bar{\omega}_e$, of $(1520 \pm 40) \text{ cm}^{-1}$ to be determined for $NF^+(X^2\Pi)$. Also, use of the vibrational component intensities in each band, together with a Franck-Condon analysis (Dyke *et al.* 1979, 1982*c*; Dyke 1987), allows the equilibrium bond length in the ion to be determined as $(1.180 \pm 0.006) \text{ \AA}$ †. As expected because both the ionizations, $NF^+(X^2\Pi) \leftarrow NF(X^3\Sigma^-)$ and $NF^+(X^2\Pi) \leftarrow NF(a^1\Delta)$, correspond to removal of an electron from the outermost orbital, an antibonding π molecular orbital, the vibrational constant, $\bar{\omega}_e$, in the ion is greater than that in the neutral states ($X^3\Sigma^-$ and $a^1\Delta$) and the equilibrium bond length in the ion is lower than the neutral molecule values.

Assignment of the NF bands shown in figure 1 was achieved on the basis of a number of pieces of evidence.

(a) Both bands were clearly associated with ionization of a short-lived molecule as increasing the mixing distance above the photoionization point above 5 cm (the optimum value for producing maximum signal intensity) i.e. increasing the reaction time, produced a dramatic decrease in intensity.

(b) The separation of the first components in each band was in good agreement with the

† $1 \text{ \AA} = 10^{-10} \text{ m} = 10^{-1} \text{ nm}$.

known separation of the zeroth vibrational levels in the $a^1\Delta$ and $X^3\Sigma^-$ neutral states, as determined from the $a^1\Delta-X^3\Sigma^-$ NF emission spectrum (Jones 1967).

(c) The experimental vertical ionization energies are in good agreement with those computed by using *ab initio* molecular-orbital calculations for each state (see table 1).

Table 1 shows ΔSCF (self-consistent field) vertical ionization energies that were obtained by performing separate SCF calculations, by using a gaussian basis set of triple-zeta plus polarization

TABLE 1. COMPUTED FIRST VERTICAL IONIZATION ENERGIES (ELECTRONVOLTS) OF $\text{NF}(X^3\Sigma^-)$ AND $\text{NF}(a^1\Delta)$

initial state	ionic state	ΔSCF value	$\Delta\text{SCF} + \text{CI}$ value	experimental value
$X^3\Sigma^-$	$^3\Pi$	13.19	12.51	12.63
$a^1\Delta$	$^3\Pi$	11.31	10.82	11.21

quality, on the neutral molecule and ion at the experimental geometry of the neutral molecule. As can be seen from this table, the ΔSCF values are higher than the experimental values indicating that unusually the correlation energy in the $\text{NF}^+(X^2\Pi)$ state is greater than in the neutral-molecule initial state. However, in line with this interpretation, when correlation energy is allowed for from extensive configuration interaction calculations, the ΔSCF values are corrected downwards giving good agreement with experimental values. This effect has also been observed in recent independent calculations on NF and NF^+ (Bettendorff & Peyerimhoff 1985).

A similar reaction sequence could also be used to produce the NCl molecule, a molecule that is valence isoelectronic with O_2 . The obvious route would be via the $\text{Cl} + \text{HN}_3$ reaction to give N_3 , followed by the reaction of chlorine atoms with N_3 to give NCl. This approach was tried and found to give very little reaction, and no photoelectron bands were seen that could be associated with the NCl molecule. However, inspection of known rate constants for these reactions (Pritt & Coombe 1980) shows that the rate constant for the $\text{Cl} + \text{HN}_3$ reaction is at least one order of magnitude smaller than the rate constant for the $\text{F} + \text{HN}_3$ reaction, whereas the $\text{Cl} + \text{N}_3$ reaction has a rate constant at room temperature that is an order of magnitude larger than that for the $\text{F} + \text{HN}_3$ reaction. As a result, the following 'hybrid' reaction scheme was used to produce the NCl molecule



Part of the HeI photoelectron spectrum obtained from these reactions is shown in figure 2. This shows contributions from hydrazoic acid, a reactant, and ethyl bromide, which was added as a calibrant, as well as three components of a vibrational series in the 9.5–10.5 eV ionization energy region with a vertical ionization energy of (9.82 ± 0.01) eV. This band was only observed when N_3 , F atoms and Cl atoms were present and studies of the intensity of this band as a function of reaction time show clearly that it is associated with a short-lived molecule. Furthermore, analysis of the vibrational separations in the observed band gave $\omega_e = (1180 \pm 30)$ cm^{-1} in the ionic state compared with values of $\bar{\omega}_e$ in $\text{NCl } X^3\Sigma^-$ and $\text{NCl } a^1\Delta$ of 827 and 905 cm^{-1} respectively (Huber & Herzberg 1979; Pritt *et al.* 1981). The observed value of $\bar{\omega}_e$ in the ion is therefore greater than the NCl neutral values, consistent with ionization from the outermost molecular orbital, which is antibonding in character.

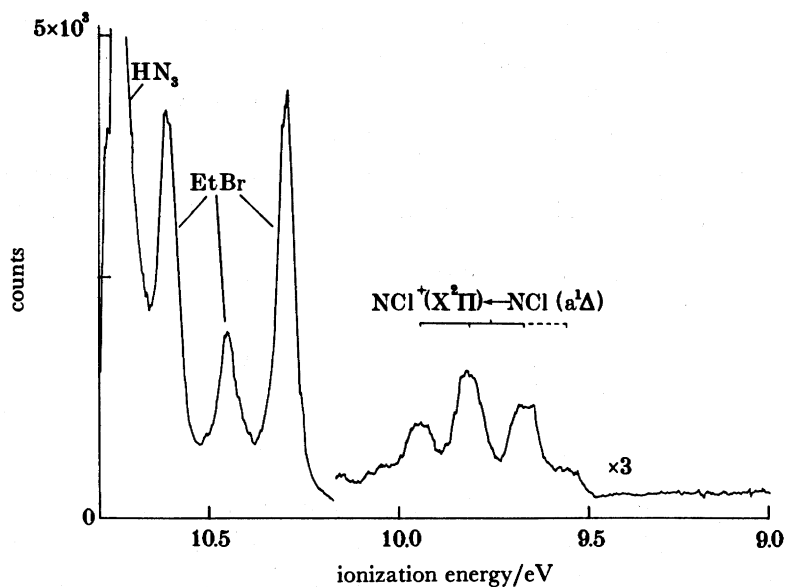


FIGURE 2. Part of the HeI photoelectron spectrum observed for the $\text{Cl} + \text{N}_3$ reaction.

Although these observations are consistent with assignment of the band at 9.82 eV to ionization of NCl, unlike the NF case only one band was observed despite the fact that the $\text{Cl} + \text{N}_3$ reaction is sufficiently exothermic to populate the $^1\Delta$ and $^3\Sigma^-$ states (Clyne & MacRobert 1983). One obvious interpretation is that the observed band is caused by the $\text{NCl}^+(\text{X}^2\Pi) \leftarrow \text{NCl}(\text{a}^1\Delta)$ ionization with the corresponding $\text{NCl}^+(\text{X}^2\Pi) \leftarrow \text{NCl}(\text{X}^3\Sigma^-)$ band being masked by more intense bands in the 10.5–11.5 eV region.

To test this hypothesis, *ab initio* calculations that include the effects of electron correlation were performed for NCl and NCl^+ by using the approach adopted previously for NF and NF^+ . The results of these calculations are shown in table 2. Again, as in the NF case, the Δ_{scf} vertical ionization energy for the $\text{NCl}^+(\text{X}^2\Pi) \leftarrow \text{NCl}(\text{a}^1\Delta)$ ionization is too high, suggesting that the correlation energy in the ion is greater than that in the neutral molecule. However, allowing for correlation energy in each state via extensive configuration interaction calculations brings the computed $\text{NCl}^+(\text{X}^2\Pi) \leftarrow \text{NCl}(\text{a}^1\Delta)$ vertical ionization energy in good agreement with experiment.

TABLE 2. COMPUTED FIRST VERTICAL IONIZATION ENERGIES (ELECTRONVOLTS) OF $\text{NCl}(\text{X}^3\Sigma^-)$ AND $\text{NCl}(\text{a}^1\Delta)$

initial state	ionic state	Δ_{scf} value	$\Delta_{\text{scf}} + \text{ci}$ value	experimental value
$\text{X}^3\Sigma^-$	$^2\Pi$	12.08	11.33	—
$\text{a}^1\Delta$	$^2\Pi$	10.33	9.84	9.82

The calculated vertical ionization energies shown in table 2 support the hypothesis that the $\text{NCl}^+(\text{X}^2\Pi) \leftarrow \text{NCl}(\text{a}^1\Delta)$ ionization has been observed and that the $\text{NCl}^+(\text{X}^2\Pi) \leftarrow \text{NCl}(\text{X}^3\Sigma^-)$ ionization is not seen because it is overlapped by the more intense bands in the 10.5–11.5 eV region.

As in the NF case, the vibrational component intensities in the observed NCl band can be

used with a series of Franck–Condon factor calculations to determine the decrease in equilibrium bond length on ionization as (0.09 ± 0.01) Å. Unfortunately, it appears that the equilibrium bond length in $\text{NCl}(a^1\Delta)$ has not been determined experimentally and as a result it is not possible to calculate the equilibrium bond length, r_e , in $\text{NCl}^+(X^2\Pi)$.

The low ionization-energy part of the photoelectron spectrum of PF, a molecule that is valence isoelectronic with oxygen, is also similar to that observed for NCl. For PF, the neutral molecule has been produced as a secondary product of the $\text{F} + \text{PH}_3$ reaction and the first band attributable to ionization of this molecule at a vertical ionization energy of (9.74 ± 0.01) eV (Dyke *et al.* 1982*c*; see figure 3) is assigned on the basis of *ab initio* calculations that include the

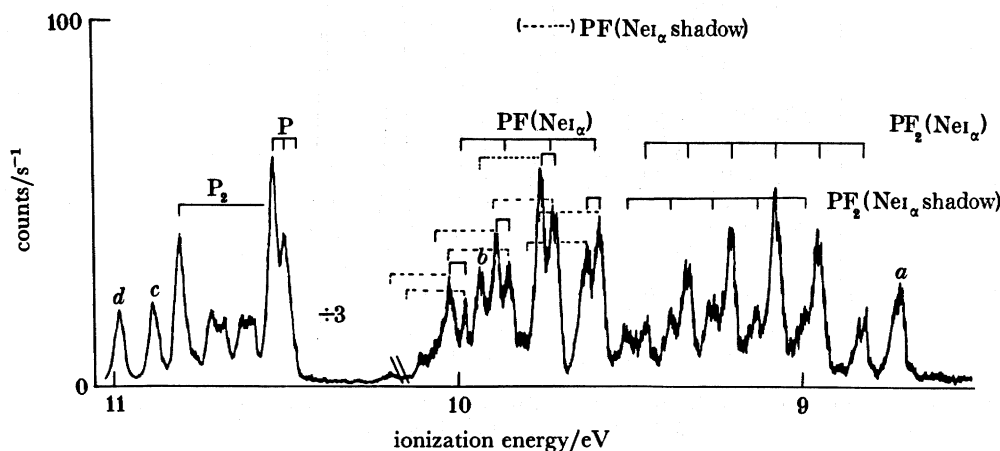


FIGURE 3. The Ne I photoelectron spectrum of the first band of PF. Bands labelled *a*, *c* and *d* are obtained by ionization of helium. The PF is produced as a secondary product of the $\text{F} + \text{PH}_3$ reaction. Bands: *a*, He ionized by NeII (32.68 eV); *b*, PF ($\text{NeI}\alpha$ shadow of second component); *c*, He ionized by NeII (30.54 eV); *d*, He ionized by NeII (30.45 eV).

effects of electron correlation to the $\text{PF}^+(X^2\Pi) \leftarrow \text{PF}(X^3\Sigma^-)$ ionization. Again, as in the NF and NCl examples, the vibrational constant, $\bar{\omega}_e$, determined for the ionic state from the experimental vibrational component separations is greater than that in the neutral molecule. The measured value in $\text{PF}^+(X^2\Pi)$ is (1030 ± 30) cm^{-1} compared with the corresponding value in the $\text{PF}(X^3\Sigma^-)$ state of 847 cm^{-1} (Huber & Herzberg 1979), and the use of the vibrational component intensities via a series of Franck–Condon calculations allows the equilibrium bond length in the ion to be determined as (1.498 ± 0.005) Å. Also as shown in figure 3, each vibrational component in the $\text{PF}^+(X^2\Pi) \leftarrow \text{PF}(X^3\Sigma^-)$ band is resolved into two parts. This arises from spin–orbit splitting in the $\text{PF}^+(X^2\Pi)$ state and the measured average value for this separation, (316 ± 16) cm^{-1} , is in good agreement with a value of 324 cm^{-1} determined in a study of the $\text{PF}^+(A^2\Sigma^+) \rightarrow \text{PF}^+(X^2\Pi)$ emission spectrum (Douglas & Frackowiak 1966).

HNO is a triatomic molecule that is isoelectronic with O_2 . It can be conveniently prepared in the gas phase by the reaction of fluorine atoms with hydroxylamine, NH_2OH , and part of the photoelectron spectrum obtained from this reaction recorded at a reagent-mixing distance of 1 cm above the photon beam is shown in figure 4. As well as some residual hydroxylamine, this spectrum shows the first band of nitric oxide, a reaction product, as well as two other bands that were also found to be associated with reaction products; a sharp intense band at (10.77 ± 0.01) eV and a broad, structured series with a vertical ionization energy of

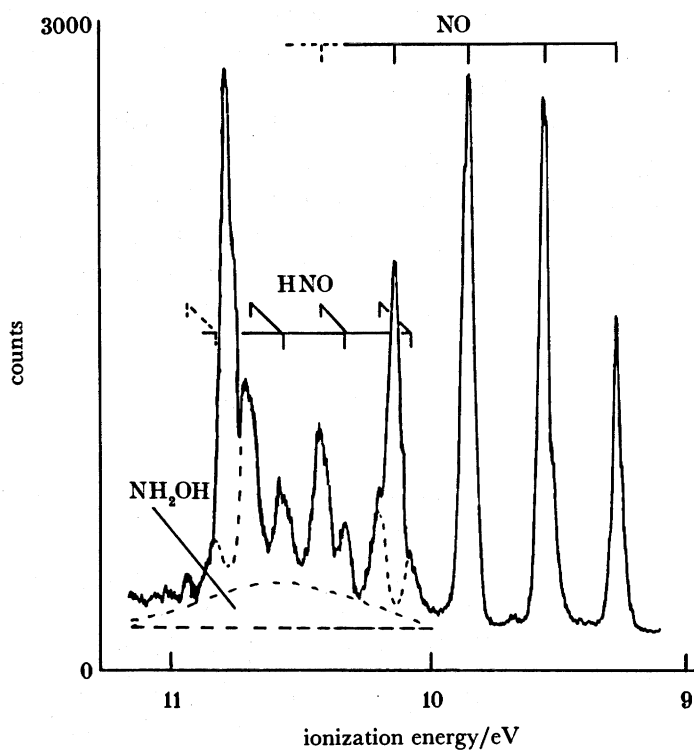


FIGURE 4. Part of the He I photoelectron spectrum recorded for the $F + \text{NH}_2\text{OH}$ reaction at a mixing distance of 1 cm above the photon beam.

(10.68 ± 0.01) eV. When the intensities of these bands were investigated as a function of reaction time, both bands were found to be associated with reactive intermediates, but the band at 10.77 eV was found to be associated with a much shorter-lived molecule than the band at 10.68 eV. On the basis of this evidence the broad band centred at 10.68 eV is assigned to the first ionization of HNO and the band at 10.77 eV is tentatively assigned to ionization of HNOH. The assignment of the 10.68 eV band to HNO is a lot firmer than the assignment of the band at 10.77 eV as the adiabatic ionization energy of the 10.68 eV band, measured as (10.07 ± 0.03) eV, is in reasonably good agreement with the first adiabatic ionization energy of HNO of (10.29 ± 0.14) eV determined by electron-impact mass spectrometry (Kohout & Lampe 1966). Also, the observed vibrational structure in this band can be assigned to excitation of the N–O stretching mode and the HNO deformation mode in the ion; the N–O stretching frequency is increased over the corresponding value in the neutral molecule, $\text{HNO}(\text{X}^1\text{A}')$, as expected by analogy with oxygen, as ionization occurs from a molecular orbital that is antibonding in the N–O direction, whereas the deformation frequency is decreased from the value in $\text{HNO}(\text{X}^1\text{A}')$. The measured average separations are (1940 ± 40) cm^{-1} for the N–O stretch and (880 ± 40) cm^{-1} for the deformation mode whereas the corresponding values in $\text{HNO}(\text{X}^1\text{A}')$ are 1556 cm^{-1} (ν_2) and 1501 cm^{-1} (ν_3) (Johns *et al.* 1983). These changes in vibrational frequencies on ionization are consistent with the equilibrium geometry change between $\text{HNO}(\text{X}^1\text{A}')$ and $\text{HNO}^+(\text{X}^2\text{A}')$ expected from *ab initio* molecular-orbital calculations (Bruna 1980; Bruna & Marian 1979).

As well as investigating reactive intermediates by single-photon ionization, it is also possible

to investigate molecules of this type by multiphoton ionization. By recording the total ion-current as a function of laser wavelength it is possible to probe the spectroscopic properties of resonant intermediate states whereas by recording a photoelectron spectrum at a fixed laser wavelength, it is possible to probe the spectroscopic properties of the ion. A very simple spectrometer has been constructed with a borrowed excimer pumped dye laser to demonstrate that short-lived molecules can be investigated in this way.

An MPI (multi-photon ionization) ion-current spectrum recorded for discharged oxygen, and tentatively assigned to $O_2(^1\Delta_g)$, has been recorded in the wavelength range 455.0–430.0 nm. The linewidth of the spectrum was controlled by the Doppler effect and the laser linewidth. Although photoelectron spectra at selected laser wavelengths need to be recorded and the laser power dependence of the observed signals needs to be investigated, the experimental ion spectrum is currently being analysed in terms of a (3+1) ionization process via a number of as-yet unobserved singlet Rydberg states of oxygen. The use of this study lies in the fact that MPI studies on $O_2(X^3\Sigma_g^-)$ have the ability to probe excited triplet states accessible from the ground $^3\Sigma_g^-$ state (Katsumata *et al.* 1986), whereas similar studies on $O_2(^1\Delta_g)$ have the advantage in that singlet excited states can be probed, for which much less experimental information is currently available. More generally, this approach is valuable in that photoelectron spectra can be recorded at selected laser wavelengths and, as a result, simplified vibrational structure will usually be seen compared with that observed in a single photon spectrum. This arises because highly excited states of neutrals often have similar equilibrium geometries and spectroscopic constants to the ground state of the positive ion. Hence short vibrational series will usually be seen in the experimental photoelectron spectra. By preparing different vibronic excited intermediate states, different vibrational frequencies will be excited in the ion. Hence in a polyatomic free radical such as the phenyl radical, where the structure in the single photon photoelectron spectrum is very complex (Butcher *et al.* 1987), it should be possible to observe considerably simplified structure. It should also be possible to determine the fundamental frequencies of a number of modes of the ion simply by preparing different highly excited vibronic states for ionization.

As well as having interests in reactive intermediates produced in the gas phase by microwave discharge or rapid atom-molecule reactions, we also have interests in molecules produced by high-temperature evaporation. Evaporation temperatures of up to 2800 K have been achieved by using a radiofrequency induction heating method (Morris *et al.* 1986). The main areas of investigation have centred on the study of metals, metal oxides and metal hydroxides.

Recently, the HeI photoelectron spectra of all the first-row transition metals has been studied (Dyke *et al.* 1985*a*). These elements were investigated firstly as possible precursors of transition-metal oxides in the vapour phase and secondly to obtain the 4s:3d photoionization cross sections in these elements to provide reliable data to be used in the interpretation of intensities of bands recorded in the photoelectron spectra of transition-metal compounds, notably metal oxides. It has been found that the 4s:3d cross-section ratio at the HeI photon energy is very low at scandium and titanium, but it increases fairly regularly to copper and zinc. As an example of a typical spectrum, figure 5 shows the HeI photoelectron spectrum of vanadium (Dyke *et al.* 1985*a*).

In this diagram, bands B and C are $(4s)^{-1}$ ionizations of the ground state of atomic vanadium whereas band E is a $(3d)^{-1}$ ionization of the ground state. Measurement of the relative band intensities allows the 4s:3d photoionization cross-section ratio of vanadium to be determined

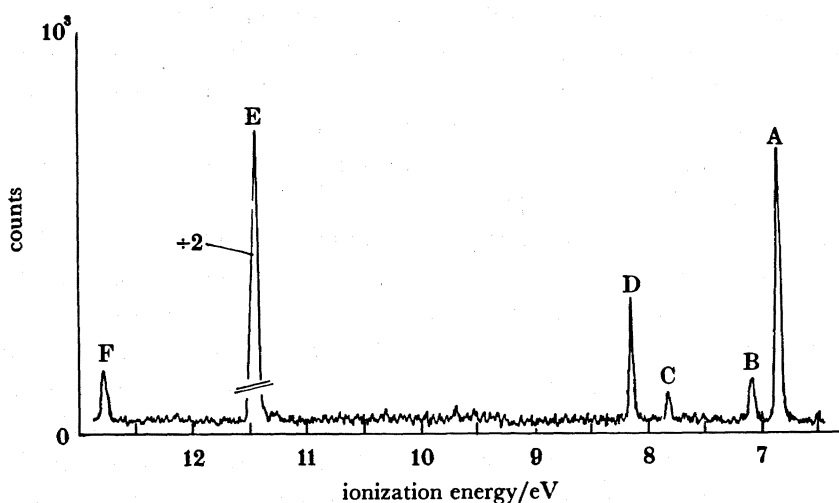


FIGURE 5. The HeI photoelectron spectrum of atomic vanadium.

at the HeI photon energy as $1 : (29.8 \pm 2.5)$, indicating that the 3d cross section is much greater than the 4s cross section. Bands A and D in figure 5 cannot be assigned to ground-state ionizations and are $(3d)^{-1}$ ionizations of an excited state of vanadium, approximately 2200 cm^{-1} above the ground state. The relative A:B band-intensity ratio can be used with the previously calculated 4s:3d cross-section ratio to give an effective beam temperature at the point of photoionization of 1940 K, which is slightly less than the furnace temperature used for evaporation of the metal of $(2030 \pm 30) \text{ K}$. This is typical of all the transition metals studied where the beam temperature at the point of photoionization, as evaluated from atomic band intensities, is several hundred degrees below the furnace temperature.

Metal oxides can also be generated in the vapour phase by direct evaporation and knowledge

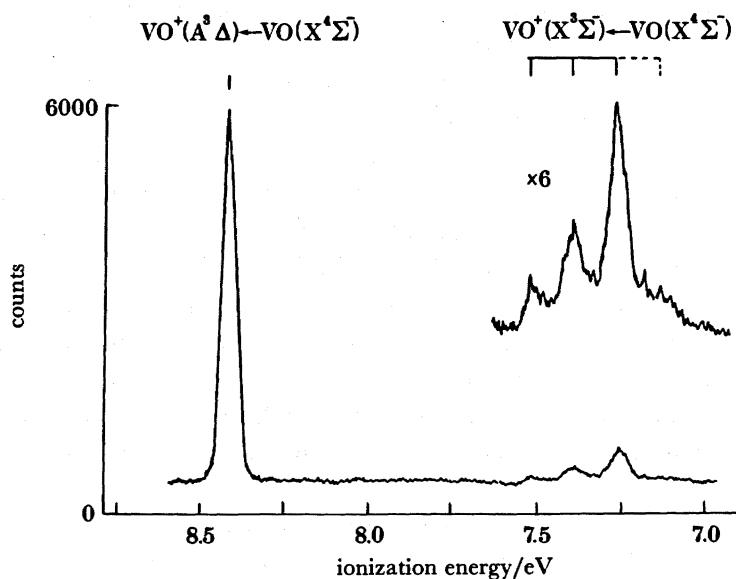


FIGURE 6. The 7.0–9.0 eV ionization energy region of the HeI photoelectron spectrum of VO.

of the photoelectron spectrum of the appropriate transition metal is very important in assigning the experimental spectrum. For example, vanadium monoxide can be obtained in the vapour phase by vaporizing stoichiometric vanadium monoxide ($\text{VO}(\text{s})$) from a tungsten furnace at 2000 K (Dyke *et al.* 1985*b*). The spectrum obtained in the 7.5–8.5 eV ionization energy region is shown in figure 6. The first band of VO, shown in this figure, is essentially a metal (4s)⁻¹ ionization whereas the second band is essentially a metal (3d)⁻¹ ionization, and this explains qualitatively why the first band is much weaker than the second. This assignment has been derived from the results of Hartree–Fock–Slater calculations and *ab initio* molecular-orbital calculations performed on the ground state of VO, the $\text{X}^4\Sigma^-$ state, and the two lowest-lying ionic states obtained by one-electron ionization from the neutral molecule. As can be seen from figure 6, the first band shows clear vibrational structure whereas the second band shows only one vibrational component. Measurement of the vibrational separations in the first band of VO allows the vibrational constant, $\bar{\omega}_e$, to be determined as $(1060 \pm 40) \text{ cm}^{-1}$ in the ground state of VO^+ , the $\text{X}^3\Sigma^-$ state, and use of the vibrational component intensities, via a series of Franck–Condon calculations, allows the equilibrium bond length in the ion to be determined as $(1.54 \pm 0.01) \text{ \AA}$.

As an example of our recent interest in metal hydroxides, the photoelectron spectra of sodium hydroxide will be briefly discussed (Dyke *et al.* 1986). For this hydroxide, mass-spectrometric studies have shown that in the temperature range 600–700 K, dimers are a major vapour-phase constituent and, in view of this, superheating beams of this hydroxide at temperatures up to 300 K higher than the furnace temperature has been used with the aim of simplifying the spectra obtained and obtaining the photoelectron spectrum of the monomer.

The He I photoelectron spectrum obtained for sodium hydroxide heated in a silver-lined carbon furnace at $(720 \pm 50) \text{ K}$ is shown in figure 7*a* and the spectrum obtained with super-

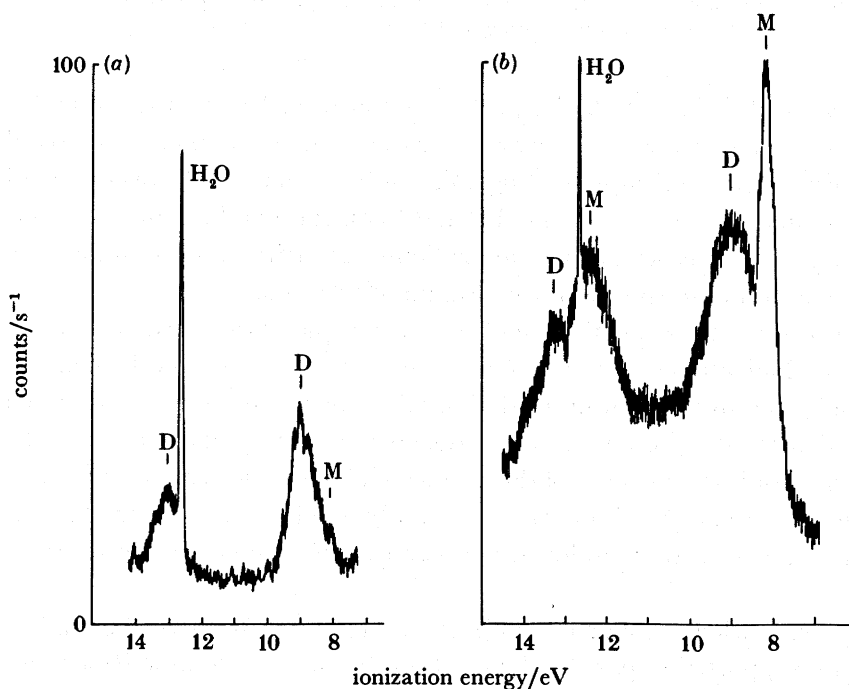


FIGURE 7. The He I photoelectron spectrum of NaOH recorded (a) without superheating and (b) with superheating.

heating is shown in figure 7*b*. On the basis of these spectra, bands marked M are assigned to ionizations of the monomer whereas the bands marked D are assigned to ionization of the dimer, as superheating is expected to increase the relative partial pressure of the monomer relative to the dimer. Also, from the results of *ab initio* molecular-orbital calculations the two observed monomer bands are assigned to ionization from the outermost π and σ monomer molecular orbitals.

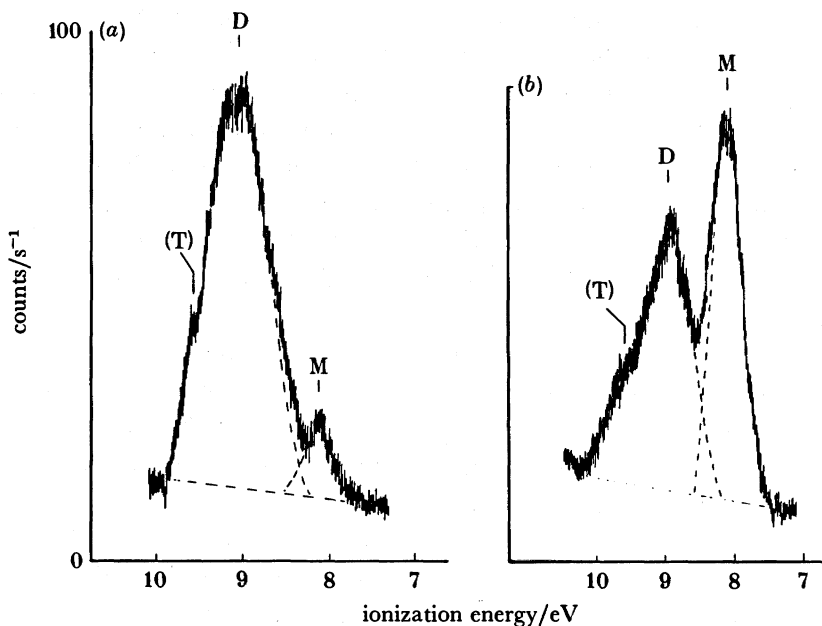


FIGURE 8. The 7.0–11.0 eV ionization-energy region of the He I photoelectron spectrum of NaOH recorded (a) without superheating and (b) with superheating.

An expanded view of the 7.0–10.0 eV spectral region recorded for sodium hydroxide with and without superheating is shown in figure 8. As can be seen, the monomer first band increases relative to that of the dimer on superheating. Also, a band marked T was observed that was found to be independent of the bands marked D and M on varying the experimental conditions, and this band was tentatively assigned to ionization of the trimer. Very similar spectra have been obtained for lithium and potassium hydroxide (Dyke *et al.* 1986).

From these spectra, perhaps one of the most important pieces of information to be obtained is the first adiabatic ionization energy of the monomer and this leads via the heat of formation of the neutral molecule, to the heat of formation of the metal-hydroxide cation. This in turn can be used to calculate the proton affinity of the corresponding alkali-metal oxide. It is also notable that the first ionization energy of the alkali-metal hydroxides appears to increase as the cluster size increases. Although this effect has been observed previously for alkali halides, the more common trend is a decrease in ionization energy with increasing cluster size.

We gratefully acknowledge financial support for this work from SERC and the CEGB. This work was also supported in part by the Air Force Office of Scientific Research (grant no. AFOSR-83-0283) through the European Office of Aerospace Research (EOARD), United States Air Force.

REFERENCES

- Bettendorff, M. & Peyerimhoff, S. D. 1985 *Chem. Phys.* **99**, 55.
 Bruna, P. J. 1980 *Chem. Phys.* **49**, 39.
 Bruna, P. J. & Marian, C. M. 1979 *Chem. Phys.* **37**, 425.
 Butcher, V., Costa, M. L., Dyke, J. M., Ellis, A. R. & Morris, A. 1987 *Chem. Phys.* **115**, 261.
 Clyne, M. A. A. & MacRobert, A. J. 1983 *J. chem. Soc. Faraday Trans. II* **79**, 283.
 Douglas, A. E. & Frackowiak, M. 1966 *Can. J. Phys.* **45**, 1074.
 Dyke, J. M. 1987 *J. chem. Soc. Faraday Trans. II* **83**, 69.
 Dyke, J. M., Feher, M. & Morris, A. 1986 *J. Electron. Spectrosc. rel. Phen.* **41**, 343.
 Dyke, J. M., Gravenor, B. W. J., Hastings, M. P., Josland, G. D. & Morris, A. 1985a *J. Electron. Spectrosc. rel. Phen.* **35**, 65.
 Dyke, J. M., Gravenor, B. W. J., Hastings, M. P. & Morris, A. 1985b *J. phys. Chem.* **89**, 4613.
 Dyke, J. M., Lewis, A. E., Jonathan, N. & Morris, A. 1982a *J. chem. Soc. Faraday Trans. II* **78**, 1445.
 Dyke, J. M., Lewis, A. E., Jonathan, N. & Morris, A. 1982b *Molec. Phys.* **47**, 1231.
 Dyke, J. M., Morris, A. & Jonathan, N. 1979 *Electron spectroscopy: theory, techniques and applications*, vol. 3, p. 189. New York: Academic Press.
 Dyke, J. M., Morris, A. & Jonathan, N. 1982c *Int. Rev. phys. Chem.* **2**, 3.
 Huber, K. P. & Herzberg, G. 1979 *Molecular spectra and molecular structure. IV. Constants of diatomic molecules*. New York: Van Nostrand.
 Jonathan, N., Morris, A., Okuda, M., Ross, K. J. & Smith, D. J. 1974 *J. chem. Soc. Faraday Trans. II* **70**, 1810.
 Jones, W. E. 1967 *Can. J. Phys.* **45**, 21.
 Johns, J. W. C., McKellar, A. R. W. & Weinberger, E. 1983 *Can. J. Phys.* **61**, 1106.
 Katsumata, S., Sato, K., Achiba, Y. & Kimura, K. 1986 *J. Electron. Spectrosc. rel. Phen.* **41**, 325.
 Kohout, F. C. & Lampe, F. W. 1966 *J. chem. Phys.* **45**, 1074.
 Morris, A., Dyke, J. M., Josland, G. D., Hastings, M. P. & Francis, P. D. 1986 *High Temp. Sci.* **22**, 95.
 Pritt, A. T. & Coombe, R. D. 1980 *Int. J. chem. Kinet.* **12**, 741.
 Pritt, A. T., Patel, D. & Coombe, R. D. 1981 *J. molec. Spectrosc.* **87**, 401.